[Article] www.whxb.pku.edu.cn

核壳结构 AlOOH 的制备、表征及其生长机制

吕 勇 陆文聪* 张良苗 岳宝华 尚兴付 倪纪朋
(上海大学理学院化学系, 上海 200444)

摘要: 在柠檬酸钠和硝酸铝水溶液体系中, 通过一步水热法制备了蜷缩刺猬状和核壳结构的 AlOOH 微球, 并用 X 射线衍射(XRD)、Fourier 变换红外(FTIR)光谱、扫描电镜(SEM)、透射电镜(TEM)、氮气吸脱附和光致发光等分析手段对制备的样品进行了形貌和结构表征. 对反应时间、反应物浓度等影响因素进行了研究. 实验结果表明: 反应时间和反应物柠檬酸钠的浓度对所得 AlOOH 微球结构的尺寸和形貌具有重要影响; 蜷缩刺猬状和核壳结构 AlOOH 微球都具有较大的比表面积, 分别为 171.5 和 178.6 $m^2 \cdot g^{-1}$; 不同形貌的 AlOOH 具有不同的荧光发射峰. 并初步探讨了核壳结构 AlOOH 微球的生长机制.

关键词: 水热法; 核壳结构; AlOOH; 光致发光; Ostwald ripening; 生长机制
中图分类号: O648

Synthesis, Characterization and Growth Mechanism of Core/Shell AlOOH Microspheres

LÜ Yong LU Wen-Cong* ZHANG Liang-Miao YUE Bao-Hua SHANG Xing-Fu NI Ji-Peng
(*Department of Chemistry, College of Science, Shanghai University, Shanghai 200444, P. R. China*)

Abstract: An experimental procedure is presented for the synthesis of crouching hedgehog-like and core/shell AlOOH microspheres by a one-step hydrothermal process in an aqueous solution of trisodium citrate at 200 ℃. The structure, morphology, purity and size of the products were characterized by several techniques such as X-ray diffraction (XRD), transmission electron microscopy (TEM), scanning electron microscopy (SEM), nitrogen adsorption/desorption measurement and photoluminescent (PL) analysis. The reaction time and concentrations of trisodium citrate influenced the final structures and shapes of the AlOOH microspheres. Brunauer-Emmett-Teller (BET) analyses revealed high values (171.5 and 178.6 $m^2 \cdot g^{-1}$) of the specific surface areas for the crouching hedgehog-like and core/shell AlOOH microspheres. A possible formation mechanism of core/shell AlOOH microspheres is proposed and discussed based on the reaction dynamics process and the assisted growth process. The photoluminescent spectra of these nanostructures showed different emission bands and this difference might be because of their distinct sizes and morphologies.

Key Words: Hydrothermal method; Core/shell; AlOOH; Photoluminescence; Ostwald ripening; Growth mechanism

Effectively controlling the sizes, morphologies, and structures of nanomaterials is important for the development of nanoscience and technology, especially for their applications with morphology-dependent properties. And it is fundamentally important to study of the crystal growth and morphology evolution processes and the corresponding mechanisms. Recently, oriented attachment, as a new and attractive growth mechanism, has caught much attention and is expected to open new access to more complex crystalline nanomaterials with anisotropic properties.

The core/shell nanospheres, which have high specific surface

Received: December 9, 2008; Revised: April 9, 2009; Published on Web: May 8, 2009.

*Corresponding author. Email: wclu@shu.edu.cn; Tel: +86-21-66132663.

The project was supported by the Special Nanotechnology Project of Shanghai Science and Technology Commission, China (0852nm00700) and Shanghai Leading Academic Discipline Project, China (J50101).
上海市科委纳米专项(0852nm00700)和上海市重点学科建设项目(J50101)资助

area and low density, are attracting great attention in both fundamental and industrial studies mainly due to their promising applications in medical[1], sensor[2], small containers[3], and catalyst carriers[4]. Various methods, including *in situ* syntheses[5], Kirkendall effect[6], phase separation[7], rapid quench[8], and ultrasonication[9], have been reported for the preparation of core/shell nanospheres. However, systematically manipulating the morphology and architecture of inorganic materials remains a challenge to material design.

Aluminum oxide hydroxide and alumina are widely used in industries as catalysts[10], catalyst supports[11], adsorbents[12], ceramics[13], and abrasives[14] due to their unique properties. Various morphologies of boehmite have been synthesized, such as nanospheres[15], nanofibers[16,17], nanorods[18], nanotubes[19,20], nanobelts[21], bunches of aligned boehmite nanowires[22], and flower-like three dimensional(3D) nanoarchitectures[23]. However, none was reported about synthesis of core/shell AlOOH nano- and microspheres *via* a one-step hydrothermal route.

In this paper, we reported a facile method for the preparation of core/shell AlOOH microspheres with about 2.2 μm in inner diameter and 380 nm in wall thickness *via* a one-step hydrothermal route with the assistance of trisodium citrate, and our work focused on the formation procedure and mechanism of the as-prepared core/shell AlOOH microspheres. Herein, the fabrication of core/shell AlOOH microspheres through hydrothermal method was introduced.

1 Experimental

All chemical reagents were analytical grade and purchased from Shanghai Chemical Reagent Company (China) without further purification. In a typical synthesis, 2.0 mmol of $Al(NO_3)_3 \cdot 9H_2O$ was dissolved in 40 mL deionized water with vigorous stirring. Trisodium citrate dihydrate ($Na_3C_6H_5O_7 \cdot 2H_2O$, 1.32 mmol) was added to the solution. The mixture was further stirred vigorously for 30 min. For the hydrothermal treatment at 200 ℃, the solution was transferred into a Teflonlined stainless steel autoclave (50 mL), which was sealed and heated for 24 h in an oven. Thereafter the autoclave was allowed to cool naturally to room temperature when the reaction time was finished. The white product was collected by centrifugation at 8000 $r \cdot min^{-1}$ for 5 min and washed with distilled water several times. Finally, the product was dried at 60 ℃ for 12 h before the collection for characterization.

The XRD patterns were recorded on a Japan Rigaku D/Max-RB X-ray diffractometer with Cu K_α radiation (λ=0.154178 nm). The morphologies of the samples were studied by field emission scanning electron microscopy (FE-SEM, JEOL JSM-6700F) and field emission transmission electron microscopy (TEM, JEOL JEM-2010F). Fourier transform infrared (FTIR) spectra were obtained on an AVATAR370 spectrometer. The nitrogen adsorption and desorption isotherms at 77 K were measured with a Micrometrics ASAP 3000 analyzer. Before measurement, the samples were degassed in vacuo at 200 ℃ for at least 6 h.

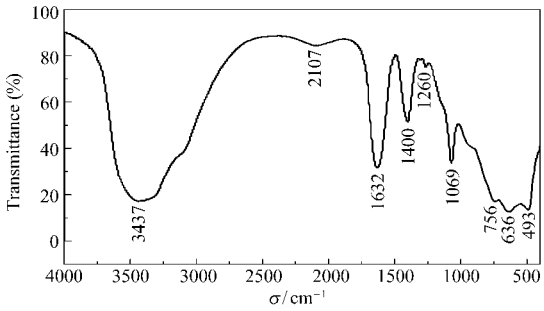

Fig.1 FTIR spectrum of the core/shell AlOOH microspheres

2 Results and discussion

2.1 Composition and morphology of the products

The crystal phase composition and purity of the products were characterized by FTIR and XRD analyses. Fig.1 showed the FTIR spectrum of the as-prepared products. The intensive band at 3437 cm^{-1} belonged to the ν_{as}(Al—O—H) stretching vibrations. The weak band at 2107 cm^{-1} was the combination band. The band at 1069 cm^{-1} and the shoulder at 1260 cm^{-1} were assigned to the δ_s(Al—O—H) and δ_{as}(Al—O—H) modes of boehmite, respectively. The three bands at 756, 636, and 493 cm^{-1} represented the vibration mode of AlO_6. The band at 1632 cm^{-1} was the feature of the bending mode of the absorbed water. These absorption bands agreed well with those reported[24].

Fig.2 shows the XRD patterns of the products synthesized after hydrothermal reaction time of 10, 24, and 48 h, respectively. The XRD patterns of the obtained samples will be discussed later in this paper. All the diffraction peaks could be readily indexed to the orthorhombic AlOOH (JCPDS Card No.21-1307) without peaks from other phases, indicating the high purity of the products. To further investigate the formation process of core/shell AlOOH microspheres, time-dependent syntheses were performed and the intermediate products at different reaction time were studied by XRD, TEM, and SEM methods.

Fig.3 shows the typical TEM images of AlOOH microstructures which were synthesized through the reaction between $Al(NO_3)_3$ and $Na_3C_6H_5O_7$ at hydrothermal condition of 200 ℃ for

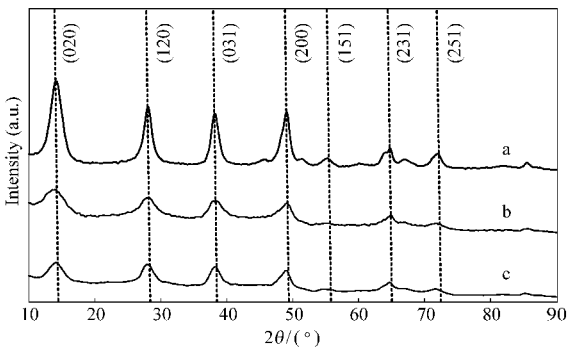

Fig.2 XRD patterns of AlOOH samples prepared at 200 ℃ for different time

t/h: (a) 10, (b) 24, (c) 48

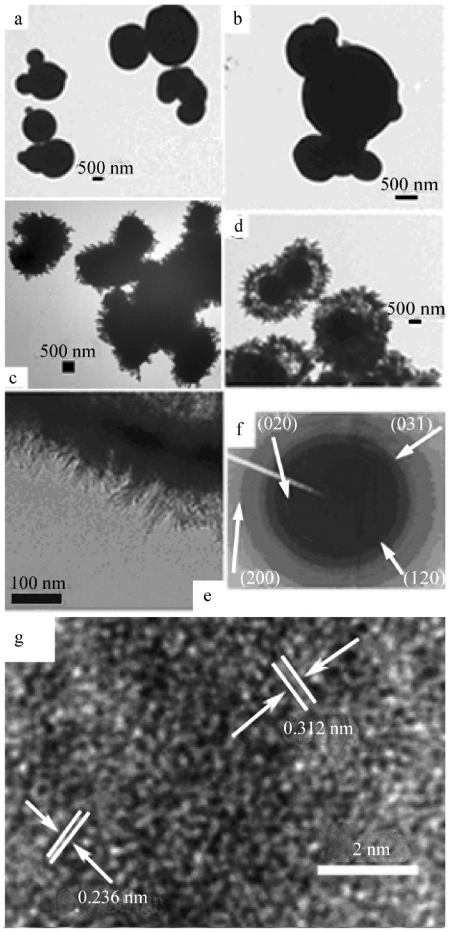

Fig.3 TEM images of the products prepared at different reaction stages at 200 ℃ (a–d), HRTEM image of outer shell (e, g) and SAED pattern of nanothorns (f)

t/h: (a) 4, (b) 10, (c) 24, (d) 48

different reaction time. When the reaction time was less than 2 h, no precipitate was formed. The microspheres (ca 1.65 μm in diameter) appeared (Fig.3a) after the reaction time extended to 4 h. As the time prolonged, the primary particles grew into bigger homoge neous microspheres (ca 2.35 μm in diameter) (Fig.3b). This could be considered as the result from the process of dissolving and re-growing of small AlOOH particles according to "Ostwald-ripening" process[25]. When the reaction time reached 24 h, the crouching hedgehog-like AlOOH microspheres with the spokewise nanothorns tapering feature (ca 100 nm in diameter in tip end, 200 nm in diameter in root end and 300−550 nm in length) were observed (Fig.3c). Interestingly, when the reaction time reached 48 h, some nanoshells grew at the top of spoke wise nanothorns (Fig.3d). A representative HRTEM image of out er shell (Fig.3e) showed clear fringes, indicating that the spokewise nanothorns were arrayed in an ordered fashion. Fig.3f is the selected area electron diffraction (SAED) patterns of a nanothorn in Fig.3e. The SAED patterns consisted of orthorhombic AlOOH with ring patterns from the (020), (120), (031) and (200) planes. It indicated that core/shell AlOOH microspheres were polycrystals. The HRTEM image (Fig.3g) indicated that the lattice distance was 0.312 and 0.236 nm, almost in accordance with the (120) and (031) lattice distance (0.316 and 0.235 nm) of the orthorhombic AlOOH crystal. This was in good agreement with the SAED observations (Fig.3f).

Fig.4a shows a typical SEM image of the AlOOH microspheres. The SEM image shown in Fig.4b displayed the crouching hedgehog-like AlOOH microspheres. As shown in Fig.4c, the core/shell AlOOH microspheres appeared. Fig.4(d, e) shows the SEM micrographs of outer shell and inner core at high magnification of core/shell AlOOH microspheres. In the XRD patterns of the samples after reacting for 10 h (Fig.3b), 24 h (Fig. 3c), and 48 h (Fig.3d), the solid microspheres (Fig.2, curve a), with better crystallinity, have much stronger and more intact diffraction peaks than those of the crouching hedgehog-like and core/shell AlOOH microspheres (Fig.2, curves b, c). As for crouching hedgehog-like and core/shell AlOOH, in respect of the special structure with the relative smaller spokewise nanothorns, nanoshells and the not-perfect crystallization[26], the diffraction peaks broaden and slightly shifted (Fig.2, curves b, c) when compared to that of the microspherical AlOOH. Hereby, we could conclude core/shell AlOOH microspheres growth mechanism.

Fig.5 illustrates the XRD patterns and Fig.6 shows the representative TEM images of the products prepared at different concentrations of trisodium citrate. All the diffraction peaks could be readily indexed to the orthorhombic AlOOH (JCPDS Card No. 21-1307). The solid microspheres (Fig.5 curve c), with better crystallinity, had much stronger and more intact diffraction peaks than those of the underdeveloped and developed cantaloupe-like AlOOH structures (Fig.5 curves a, b), which was in good agreement with the TEM images (Fig.6). As for underdeveloped and developed cantaloupe-like AlOOH, in respect of the special structure with the relative smaller nanorods and the not-perfect

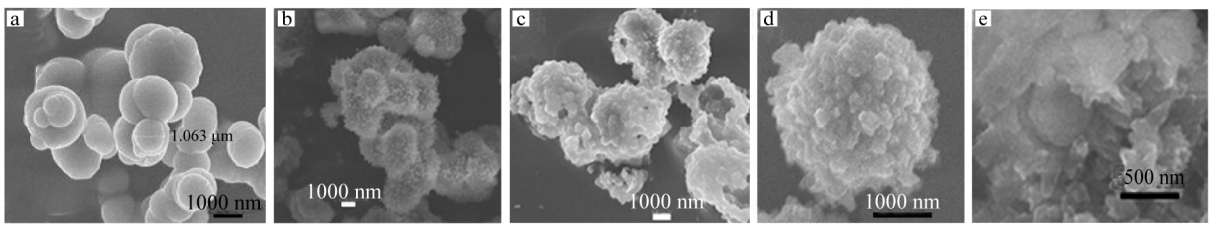

Fig.4 SEM images of products prepared at different reaction stages at 200 ℃ (a–c), high-magnification SEM images of outer shell (d) and inner core (e)

(a) AlOOH solid microspheres displayed in Fig.3a; (b) crouching hedgehog-like microspheres displayed in Fig.3c; (c) core/shell AlOOH microspheres displayed in Fig.3d

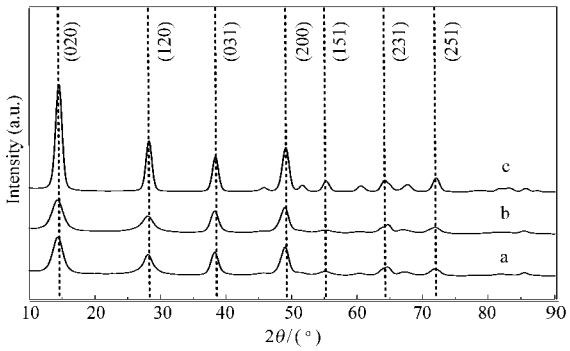

Fig.5 XRD patterns of the AlOOH samples prepared at 200 ℃ for 24 h with different amount of trisodium citrate

$n(Na_3C_6H_5O_7)$/mmol: (a) 1/8, (b) 1/2, (c) 3.0

crystallization, the diffraction peaks broadened and slightly shifted (Fig.5 curves a, b) when compared to that of the microspherical AlOOH. Fig.6a showed the irregular nanorods obtained in the absence of trisodium citrate. When 1/32 mmol trisodium citrate was added, the as-synthesized products were composed of bunches of side-by-side nanorods (Fig.6b). As the amount of trisodium citrate dihydrate reached 1/8 mmol, most of the products had underdeveloped cantaloupe-like structures (Fig.6c). The nanorods of the surface were also arrayed in an ordered fashion and closely packed together. With an increase in the dosage of trisodium citrate to 1/2 mmol, the as-synthesized product was monodispersed developed cantaloupe-like structure (Fig.6d), which had been demonstrated in detail in our previous work[27]. When the amount of trisodium citrate further increased to 3.0 mmol, the morphology of the product changed greatly and turned into microspheres with diameter of ca 2.0 μm (Fig.6e).

Nitrogen adsorption/desorption measurement was conducted to characterize the Brunauer-Emmett-Teller (BET) surface area and internal pore structure. The recorded adsorption and desorption isotherms for the crouching hedgehog-like (Fig.7a) and core/shell AlOOH microspheres (Fig.7b) showed a significant hysteresis. The isotherms were identified as type IV, which was characteristic of mesoporous materials. The BET specific surface areas of the obtained crouching hedgehog-like and core/

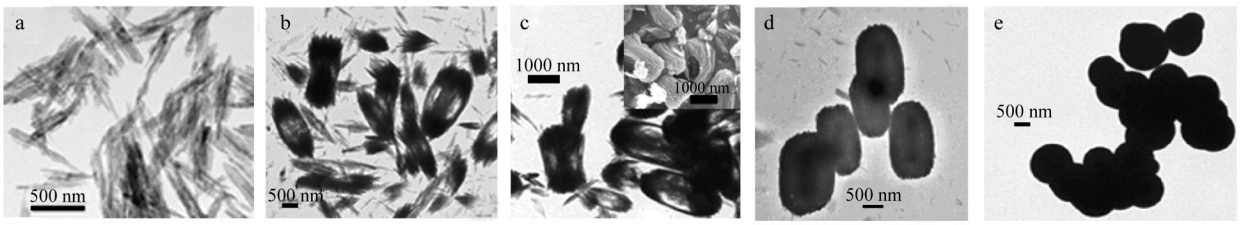

Fig.6 TEM images of samples synthesized at 200 ℃ for 24 h with different amount of trisodium citrate

$n(Na_3C_6H_5O_7 \cdot 2H_2O)$/mmol: (a) 0, (b) 1/32, (c) 1/8, (d) 1/2, (e) 3.0; Inset in Fig.c shows the corresponding SEM image.

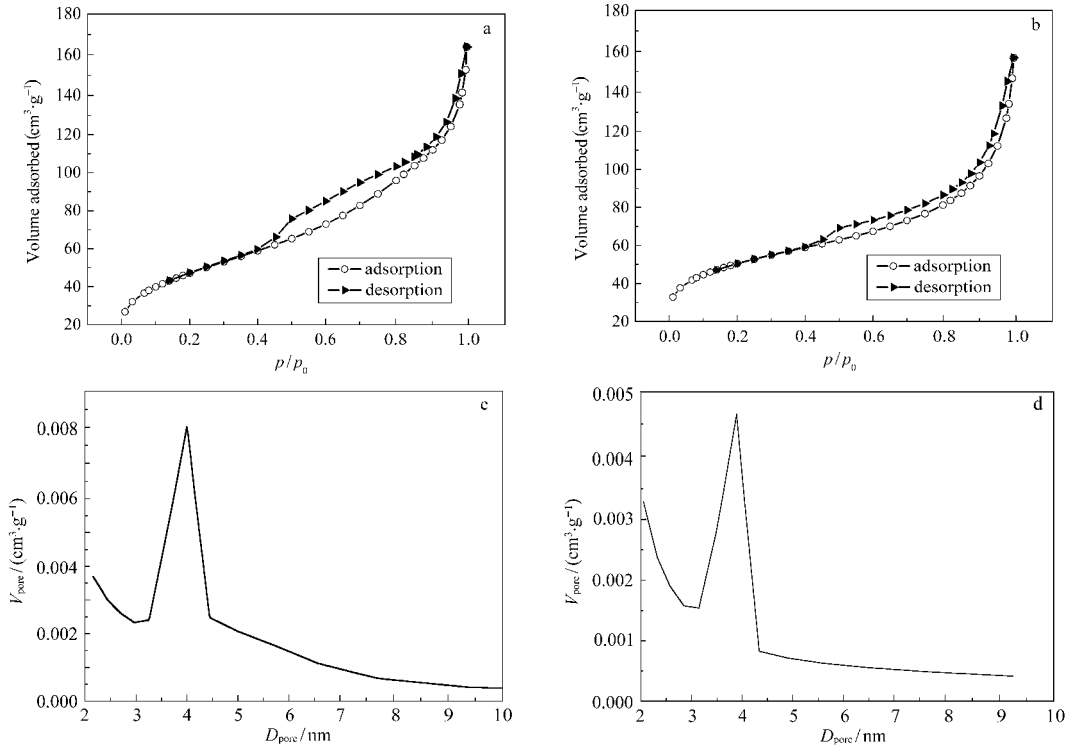

Fig.7 N_2 adsorption/desorption isotherms (a, b) and pore-size distributions (c, d) for AlOOH microspheres

(a, c) crouching hedgehog-like AlOOH microspheres; (b, d) core/shell AlOOH microspheres

shell AlOOH microsphores calculated from N_2 isotherms were about 171.5 and 178.6 $m^2 \cdot g^{-1}$, respectively. Barrett-Joyner-Halenda (BJH) calculations for the pore-size distribution, derived from desorption data, revealed narrow distribution for the crouching hedgehog-like and core/shell AlOOH microspheres centered at 4.0 and 3.9 nm (Fig.7(c, d)), respeatively. A narrow mesopore size distribution (2−8 nm) was close to the value observed by HRTEM (Fig.3e). The pores presumably arose from the spaces within a nanothorn and the internanothorns. The results displayed that the obtained crouching hedgehog-like and core/ shell AlOOH microspheres had porous properties.

To examine the size and shape dependence of optical properties of the AlOOH solid microspheres in Fig.3b and crouching hedgehog-like microspheres synthesized at 200 ℃, photoluminescent (PL) measurements were made at an excitation wavelength of 254 nm at room temperature. Fig.8a shows the PL spectrum of the AlOOH solid microspheres in Fig.3b, which has several emission bands: two broad bands at 356 and 367 nm, one sharp band at 469 nm, together with one weak shoulder at 451 nm. By sharp contrast, the corresponding PL spectrum of the crouching hedgehog-like microspheres displayed a single broad band at 362 nm (Fig.8b). The emission bands located at 356 and 367 nm in Fig.8a could be ascribed to anionic vacancies (F and F^+ centers or a combination of these two types of defects). The emission bands at 451 and 469 nm present in both Fig.8a and Fig. 8b might be attributed to the anionic vacancies of OH^-[28]. The optical difference might be due to the distinct sizes and morphologies of the AlOOH solid microspheres for 10 h and crouching hedgehog-like microspheres at 200 ℃.

2.2 Growth mechanism of the architecture

To investigate the fabrication mechanism of core/shell AlOOH microspheres, the detailed time (Figs.3 and 4) and the amount of trisodium citrate (Fig.6) course study were conducted at 200 ℃.

In the precursor solution, the $(C_6H_5O_7)^{3-}$ ions were added first to form an $Al(C_6H_5O_7) \cdot 3H_2O$ complex according to the following reaction (1)[29]. In that case, the morphology of AlOOH microstructure would be controlled by the molar ratio (r) of the Al^{3+} ions to the $(C_6H_5O_7)^{3-}$ ions in the solutions, which had been demonstrated to be a key factor in determining the morphology of 1D $BaWO_4$ nanostructures[30].

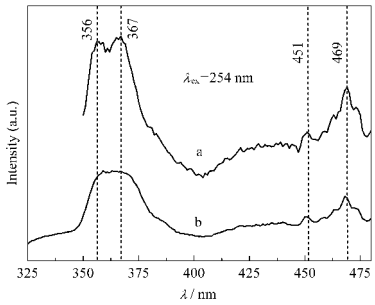

Fig.8 Room-temperature photoluminescent spectra of AlOOH microspheres

(a) AlOOH solid microspheres in Fig.2b, (b) crouching hedgehog-like microspheres prepared at 200 ℃

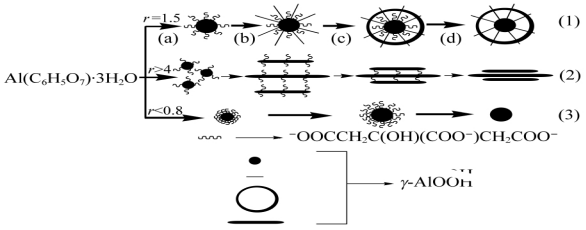

Fig.9 Schematic illustration of the formation process of (1) core/shell AlOOH microspheres (a−d), (2) cantaloupe-like AlOOH superstructures and (3) AlOOH microspheres

(a) AlOOH nucleation process; (b) spokewise nanothorn growth process; (c) outer shell growth process; (d) citrate removing process

$$Al^{3+}+(C_6H_5O_7)^{3-} \overset{H_2O}{\rightleftharpoons} Al(OOCCH_2C(OH)(COO)CH_2COO) \cdot 3H_2O \quad (1)$$

For the excess of Al^{3+} ions (r=1.5), the hydrolysis reaction took place between $Al(C_6H_5O_7) \cdot 3H_2O$ and dissociative Al^{3+} ions. We supposed that some homogeneous boehmite nanostructures were formed because the AlOOH nanoparticles were dissolved and regrown according to "Ostwald-ripening" process. And then, the AlOOH microspheres appeared. As citrate molecules cooperated selectively on the surface of AlOOH microspheres and could serve as template and site substitution agent in the synthesis[31−33], the crouching hedgehog-like microspheres with spokewise nanothorns were observed with the processes of reaction. When the reaction time reached 48 h, the excessive Al^{3+} ions hydrolyzed unceasingly, and hydrogen bonds were formed between hydroxyl of boehmite in adjacent planes of AlO_6 octahedra[34]. Accordingly, the AlOOH nanoshells self-assembled at the top of spokewise nanothorns for the effect of hydrogen bonds. And then, the core/shell AlOOH microsperes were formed, as could be seen in scheme (1) of Fig.9.

Without trisodium citrate, the Al^{3+} ions hydrolyzed and produced boehmite phase at higher temperature and pressure. Therefore, $Al(NO_3)_3$ hydrolyzed slowly to form nanoparticles at the early stage. When Al^{3+} ions was greatly excessive (r>4), few citrate molecules cooperated with Al^{3+} ions and limited anisotropic growths, allowing the hydrolysis reaction to grow along one direction to form nanorods[35]. Finally, the crystal nucleus formed rod-like structures. Hydrogen bonds were formed between carboxyl of trisodium citrate cooperating with the surface of AlOOH nanorods. This led to the nanorods self-organize into cantaloupe-like assemblies, as could be seen in scheme (2) of Fig.9.

When $(C_6H_5O_7)^{3-}$ ions were greatly excessive (r<0.8), the growth of AlOOH microspheres was limited for abundant citrate molecules cooperating with the surface of AlOOH microspheres. Therefore, only AlOOH microspheres formed in this case, which were illustrated in scheme (3) of Fig.9.

3 Conclusions

The novel crouching hedgehog-like and core/shell AlOOH microspheres have been successfully synthesized *via* a one-step hydrothermal route with the assistance of trisodium citrate. Comparative observations demonstrate that the reaction time and the concentration of trisodium citrate play important roles in the formation of AlOOH microstructures. In the appropriate case (reac tion time of 48 h and $Al^{3+}/(C_6H_5O_7)^{3-}$ molar ratio of 1.5), the obtained core/shell AlOOH microspheres are uniform and pure with the average inner diameter of 2.2 μm and outer diameter of 3.0 μm. This process for the synthesis of core/shell AlOOH microspheres has great beauty and significance for its simplicity, high efficiency and good potential for scale-up. Furthermore, the core/shell AlOOH microspheres might have potential applications in ceramic industry and other fields. The PL spectra of the AlOOH superstructures turned out to be size-dependent or morphology-dependent.

References

1 Arias, J. L.; Linares-Molinero, F.; Gallardo, V.; Delgado, A. *Eur. J. Pharmaceu. Sci.*, **2008, 33**: 252

2 Thakar, R.; Chen, Y. C.; Snee, P. T. *Nano Lett.*, **2007, 7**: 3429

3 Schellenberg, C.; Akari, S.; Regenbrecht, M.; Tauer, K.; Petrat, F. M.; Antonietti, M. *Langmuir*, **1999, 15**: 1283

4 Mei, Y.; Lu, Y.; Polzer, F.; Ballauff, M. *Chem. Mater.*, **2007, 19**: 1062

5 Kou, H.; Pan, Y. B.; Guo, J. K. *Ceram. Int.*, **2007, 33**: 305

6 Gao, J. H.; Liang, G. L.; Zhang, B.; Kuang, Y.; Zhang, X. X.; Xu, B. *J. Am. Chem. Soc.*, **2007, 129**: 1428

7 Harada, A.; Kataoka, K. *Science*, **1999, 65**: 283

8 Li, Y. L.; Ishigaki, T. *Chem. Phys. Lett.*, **2003, 367**: 561

9 Geng, J.; Liu, B.; Xu, L.; Hu, F. N.; Zhu, J. J. *Langmuir*, **2007, 23**: 10286

10 Doskocil, E. J.; Mueller, G. M. *J. Catal.*, **2005, 234**: 143

11 Yan, W. F.; Ma, Z.; Mahurin, S. M.; Jiao, J.; Hagaman, E. W.; Overbury, S. H.; Dai, S. *Catal. Lett.*, **2008, 121**: 209

12 Panias, D.; Krestou, A. *Powder Technol.*, **2007, 175**: 163

13 Kaya, C.; Butler, E. G. *J. Eur. Ceram. Soc.*, **2002, 22**: 1917

14 Sun, Y. L.; Zuo, D. W.; Zhu, Y. W.; Wang, M. *Chin. J. Chem. Phys.*, **2007**, **20**: 643

15 Naskar, M. K.; Chatterjee, M. *J. Am. Ceram. Soc.*, **2005, 88**: 3322

16 Zhu, H. Y.; Gao, X. P.; Song, D. Y.; Bai, Y. Q.; Ringer, S. P.; Gao, Z.; Xi, Y. X.; Martens, W.; Riches, J. D.; Frost, R. L. *J. Phys. Chem. B*, **2004, 108**: 4245

17 Kuiry, S. C.; Megen, E.; Patil, S. D.; Deshpande, S. A.; Seal, S. *J. Phys. Chem. B*, **2005, 109**: 3868

18 Tang, B.; Ge, J. C.; Zhuo, L. H.; Wang, G. L.; Niu, J. Y.; Shi, Z. Q.; Dong, Y. B. *Eur. J. Inorg. Chem.*, **2005, 21**: 4366

19 Qu, L. H.; He, C. Q.; Yang, Y.; He, Y. L.; Liu, Z. M. *Mater. Lett.*, **2005, 59**: 4034

20 Kuang, D. B.; Fang, Y. P.; Liu, H. Q.; Frommen, C.; Fenske, D. *J. Mater. Chem.*, **2003, 13**: 660

21 Gao, P.; Xie, Y.; Chen, Y.; Ye, L. N.; Guo, Q. X. *J. Cryst. Growth*, **2005, 285**: 555

22 Zhang, J.; Wei, S. Y.; Lin, J.; Luo, J. J.; Liu, S. J.; Song, H. S.; Elawad, E.; Ding, X. X.; Ga, J. M.; Qi, S. R.; Tang, C. C. *J. Phys. Chem. B*, **2006, 110**: 21680

23 Zhang, J.; Liu, S. J.; Lin, J.; Song, H. S.; Luo, J. J.; Elssfah, E. M.; Ammar, E.; Huang, Y.; Ding, X. X.; Gao, J. M.; Qi, S. R.; Tang, C. C. *J. Phys. Chem. B*, **2006, 110**: 14249

24 Kiss, A. B.; Keresztury, G.; Farkas, L. *Spectrochim. Acta A*, **1980, 36**: 653

25 Lameiras, F. S. *Mater. Res.*, **1999, 2**: 139

26 Shi, Y. H.; Chen, J.; Shen, P. W. *J. Alloys Compd.*, **2007, 441**: 337

27 Feng, Y. L.; Lu, W. C.; Zhang, L. M.; Bao, X. H.; Yue, B. H.; Lv, Y.; Shang, X. F. *Cryst. Growth Des.*, **2008, 4**: 1426

28 Yu, Z. Q.; Wang, C. X.; Gu, X. T.; Li, C. *J. Lumines*, **2004, 106**: 153

29 Kuan, W. H.; Wang, M. K.; Huang, P. M.; Wu, C. W.; Chang, C. M.; Wang, S. L. *Water Res.*, **2005, 39**: 3457

30 Shi, H.; Qi, L.; Ma, J.; Wu, N. *Adv. Funct. Mater.*, **2005, 15**: 442

31 Meyer, M.; Bée, A.; Talbot, D.; Cabuil, V.; Boyer, J. M.; Répetti, B.; Garrigos, R. *J. Colloid Interface Sci.*, **2004, 277**: 309

32 Meldrum, F. C.; Hyde, S. T. *J. Cryst. Growth*, **2001, 231**: 544

33 Liang, J. B.; Liu, J. W.; Xie, Q.; Bai, S.; Yu, W. C.; Qian, Y. T. *J. Phys. Chem. B*, **2005, 109**: 9463

34 Digne, M.; Sautet, P.; Raybaud, P.; Toulhoat, H.; Artacho, E. *J. Phys. Chem. B*, **2002, 106**: 5155

35 Yin, Y. D.; Alivisatos, A. P. *Nature*, **2005, 437**: 664